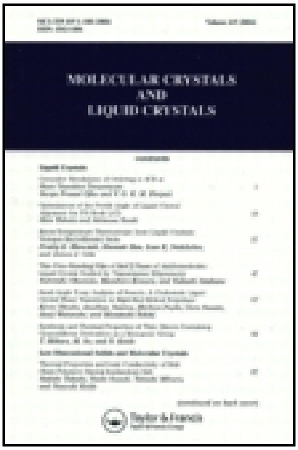

Molecular Crystals and Liquid Crystals
Publication details, including instructions for authors and subscription information:
http://www.tandfonline.com/loi/gmcl18

The Symmetry Property of a 90° Twisted Nematic Liquid Crystal Cell

A. Lien [a] , H. Takano [b] , S. Suzuki [b] & H. Uchlda [b c]

[a] IBM Research Division, Thomas J. Watson Research Center, P.O. Box 218, Yorktown Heights, NY, 10598

[b] Display Technology and Design Center, ISM Japan Ltd., Shimotsuruma, Yamatoshi Kanagawaken, Japan

[c] Current address for H. Uchida is ERATO, Kaga, Itabashi-Ku, Tokyo, Japan

Version of record first published: 24 Sep 2006.

To cite this article: A. Lien , H. Takano , S. Suzuki & H. Uchlda (1991): The Symmetry Property of a 90° Twisted Nematic Liquid Crystal Cell, Molecular Crystals and Liquid Crystals, 198:1, 37-49

To link to this article: http://dx.doi.org/10.1080/00268949108033381

Mol. Cryst. Liq. Cryst., 1991, Vol. 198, pp. 37–49
Reprints available directly from the publisher
Photocopying permitted by license only

Printed in the United States of America

The Symmetry Property of a 90° Twisted Nematic Liquid Crystal Cell

A. LIEN

IBM Research Division, Thomas J. Watson Research Center, P.O. Box 218, Yorktown Heights, NY 10598

and

H. TAKANO, S. SUZUKI and H. UCHIDA†

Display Technology and Design Center, IBM Japan Ltd., Shimotsuruma, Yamato-shi Kanagawa-ken, Japan

(Received August 15, 1990)

A set of symmetry properties of a 90° twisted nematic (TN) cell under rotation of polarizers has been observed both experimentally and theoretically for the first time. These symmetry properties can be explained by an argument based on rotation and time reversal transformations. The use of these symmetry properties allows one to answer the long time puzzle as to whether the *e*-mode TN cell, in which the transmission axis of the entrance polarizer is parallel to the entrance rubbing direction, is superior to the *o*-mode TN cell, in which the transmission axis of the entrance polarizer is perpendicular to the entrance rubbing direction, for both normally white and normally black cases. In addition, these symmetry properties provide us with a useful test for any existing TN LCD computer simulation program.

I. INTRODUCTION

The thin film transistor driving liquid crystal display (TFT/LCD) has attracted much attention, because of its good optical performance and its potential to be used in the areas such as pocket TV, high resolution projection TV, and thin and light weight computer monitor/terminals. Due to its low threshold voltage, low power consumption, and good contrast ratio, the 90° twisted nematic (TN) mode LCD has most commonly been adopted in the TFT/LCDs. For a TN panel, polarizer orientation is one of the important parameters to achieve a better optical performance, such as better contrast ratio and wider viewing angle. In this paper, we discuss, for the first time, a set of symmetry properties of a 90° twisted nematic (TN) cell under rotation of polarizers, which was discovered in the course of optimizing the polarizer orientation. Part of this symmetry was first observed experimentally. To study these symmetry properties systematically, computer sim-

†Current address for H. Uchida is ERATO, Kaga, Itabashi-Ku, Tokyo, Japan.

ulations were then performed. From the simulation results, we not only confirmed those experimentally observed symmetry properties, we also obtained a complete set of symmetry properties for the 90° TN cell. To verify the whole set of symmetry properties experimentally, more detail and careful experiments were than carried out, and thus the whole set of the symmetry properties was confirmed. Interestingly, these symmetry properties can be explained by an argument based on rotation and time reversal transformations. By the use of these symmetry properties, we will be able to clarify the long time puzzle as to whether the *e*-mode dominant TN cell (abbreviated as *e*-mode TN cell in the following discussion), in which the transmission axis of the entrance polarizer is parallel to the entrance rubbing direction, is superior to the *o*-mode dominant TN cell (abbreviated as *o*-mode TN cell in the following discussion), in which the transmission axis of the entrance polarizer is perpendicular to that of the entrance rubbing direction, for both normally white (NW) and normally black (NB) cases. In addition, these symmetry properties provide us with a useful test for any existing TN LCD computer simulation program. The arrangement of the rest of this paper is as follows. The computer simulation results and the experimental results will be presented in the sections II and III, respectively, to show the whole set of the symmetry properties.‡ The proof and discussion of these symmetry properties will be given in the section IV. A conclusion is given in section V.

II. SIMULATION RESULTS

Figure 1 shows the calculation results of the transmission versus applied voltage curves for four different viewing zones for the NB case, in which the transmission axis of the exit polarizer is parallel to that of the entrance polarizer. The left hand side is for the *e*-mode results, while the right hand side is for the *o*-mode results. Each sub-figure shows three viewing angles: 0°, 20°, and 40° with respect to the substrate normal. The calculation was carried out in two steps, as usual. In the first step, the Helmholtz free-energy density, which is the sum of the Oseen-Frank strain free-energy[1] and the electrostatic free-energy,[2] is minimized to obtained a liquid crystal director deformation profile inside the TN cell. In the second step, the faster 4 × 4 propagation matrix[3] is used to compute the transmission of that monochromatic light through the TN cell for the liquid crystal director deformation profile calculated in the first step. A theoretical polarizer model[4] based on the faster 4 × 4 propagation matrix theory for the commercially available sheet polarizer and for the glass substrate is also included in this calculation. The calculation is carried out for a 90° TN cell filled with ZLI-3771 of EM Industries, Inc. We used $k_{11} = 13.7 \times 10^{-12}$ N, $k_{22} = 7.0 \times 10^{-12}$ N, $k_{33} = 16.8 \times 10^{-12}$ N, ε (parallel) = 7.3, ε (normal) = 3.6, $n_e = 1.5965$, $n_o = 1.4920$, pretilt angle = 2°,

‡The sequence of the simulation results and the experimental results arranged in sections II and III, respectively, is just for the convenience of presentation. It does not imply that the computer simulation plays a more important role than the experiment work in the discovery of these symmetry properties. In fact, as we have already pointed out, the whole set of the symmetry properties was discovered through an interaction of experimental and theoretical efforts.

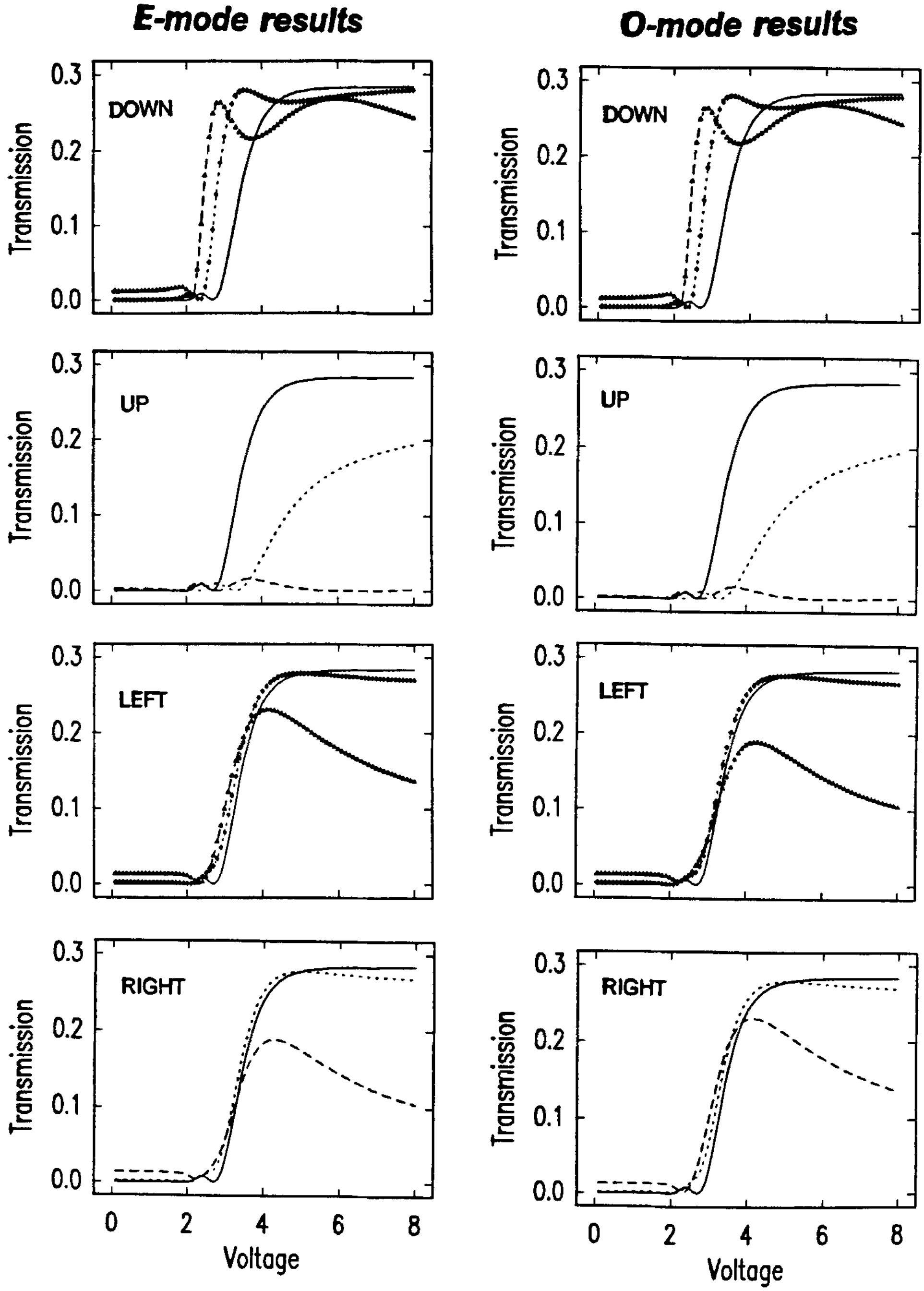

FIGURE 1 The calculated transmission versus applied voltage curves for four different viewing zones for a 90° TN cell filled with ZLI-3771 in the NB configuration. The left hand side is for the *e*-mode results, while the right hand side is for the *o*-mode results. Each sub-figure shows three viewing angles: 0° (solid line), 20° (dotted line with or without diamond symbols), and 40° (dashed line with or without triangle symbols) with respect to the substrate normal.

twist angle = 90°, cell gap thickness = 10.4 μm for liquid crystal and cell parameters; n = 1.5, d = 1.1 mm for glass parameters; and $n_o = 1.5 + i \times 5.5 \times 10^{-5}$, $n_e = 1.5 + i \times 2.2 \times 10^{-3}$, d = 190 μm for polarizer parameters. Here, $i = \sqrt{-1}$. The wavelength of the incident light is 545 nm. This figure clearly shows the following symmetries:

The *e*-mode right ⇔ The *o*-mode left,

The *e*-mode left ⇔ The *o*-mode right,

The *e*-mode up ⇔ The *o*-mode up,

The *e*-mode down ⇔ The *o*-mode down. (1)

Here, the symbol ⇔ represents the optics properties of figures on both sides are equivalent or nearly equivalent.

Figure 2 shows the calculation results for the NW case with the same liquid crystal, cell, glass, and polarizer parameters as those of the NB case, only the polarizer arrangement is different from the NB case. For the NW case, the transmission axis of the exit polarizer is perpendicular to that of the entrance polarizer. From Figure 2, we observe the following symmetries:

The *e*-mode right ⇔ The *e*-mode left,

The *o*-mode right ⇔ The *o*-mode left. (2)

III. EXPERIMENTAL RESULTS

Experimentally, we have made 90° TN cells with a cell gap thickness of 10.4 μm, pretilt angle of 2° and filled with ZLI-3771. The cell was laminated with G1220DU (Nitto Denko Co. Ltd.) polarizers. The measurement results for the NB case, corresponding to theoretical results of Figure 1 are shown in Figure 3, while measurement results for the NW case, corresponding to theoretical results of Figure 2 are shown in Figure 4. Overall, the experimental data agree reasonably well to the corresponding theoretical results. Especially, the symmetry properties given in Equation 1 are also shown in Figure 3, and the symmetry properties given in Equation 2 are also shown in Figure 4.

IV. PROOF AND DISCUSSION

These symmetry properties can be explained by the argument based on rotation and time reversal transformations as follows. Figure 5(a) shows the *e*-mode right viewing zone for the NB cell. The rubbing directions are shown with head arrows, and the transmission axes of the polarizers are shown with double head arrows. In

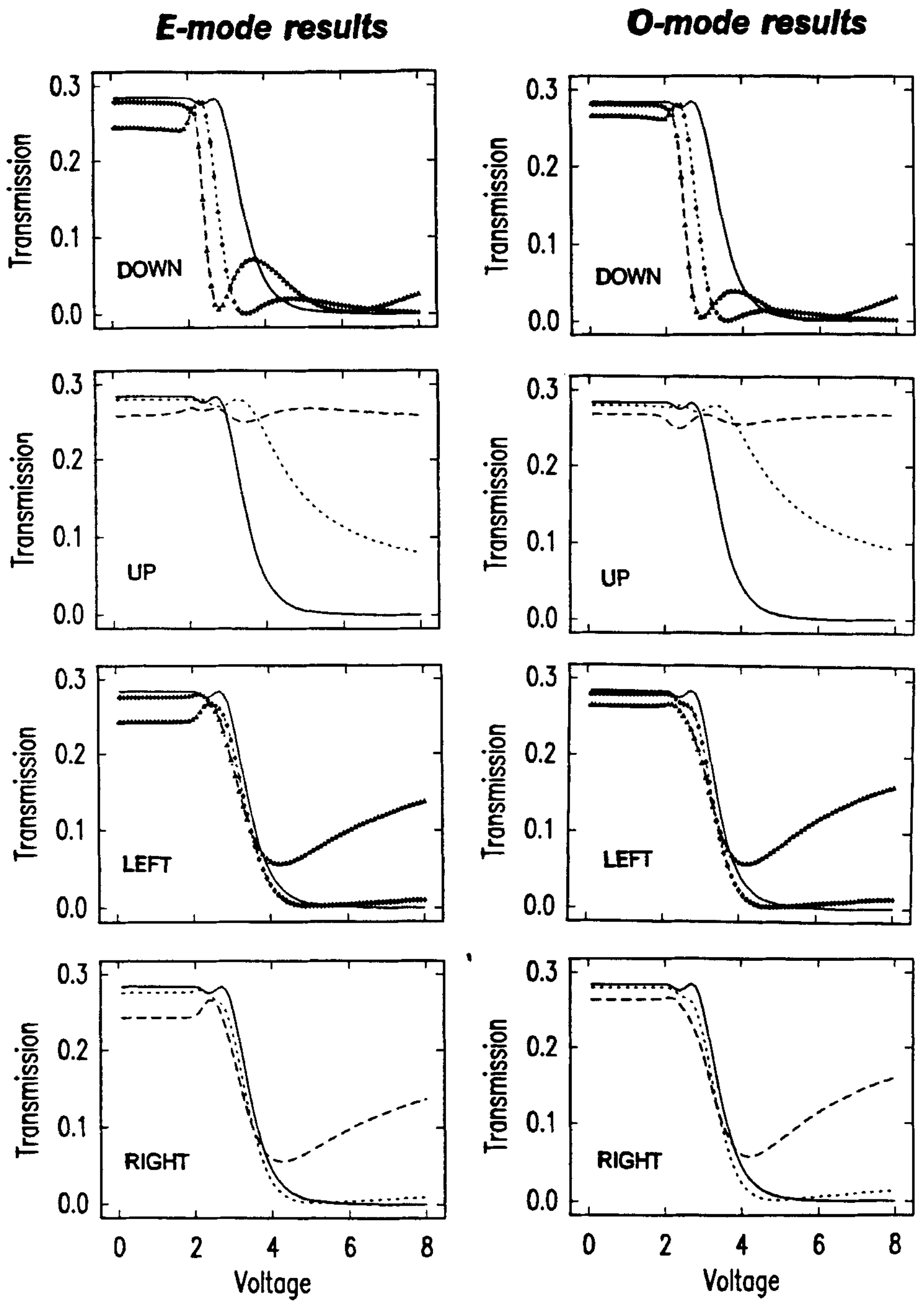

FIGURE 2 The calculated transmission versus applied voltage curves for four different viewing zones for a 90° TN cell filled with ZLI-3771 in the NW configuration. The left hand side is for the e-mode results, while the right hand side is for the o-mode results. Each sub-figure shows three viewing angles: 0° (solid line), 20° (dotted line with or without diamond symbols), and 40° (dashed line with or without triangle symbols) with respect to the substrate normal.

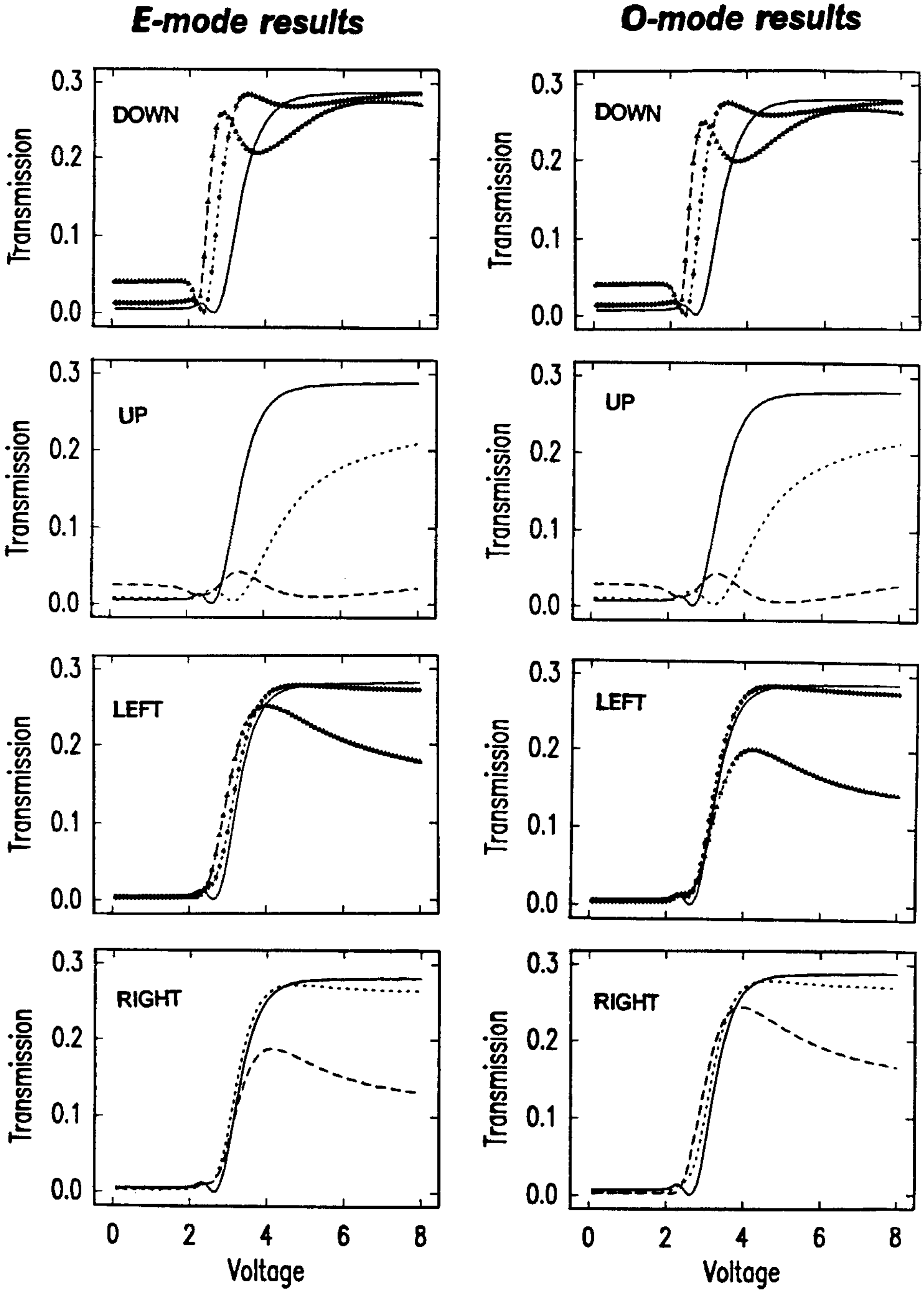

FIGURE 3 The experimental transmission versus applied voltage curves for four different viewing zones for a 90° TN cell filled with ZLI-3771 in the NB configuration. The left hand side is for the *e*-mode results, while the right hand side is for the *o*-mode results. Each sub-figure shows three viewing angles: 0° (solid line), 20° (dotted line with or without diamond symbols), and 40° (dashed line with or without triangle symbols) with respect to the substrate normal.

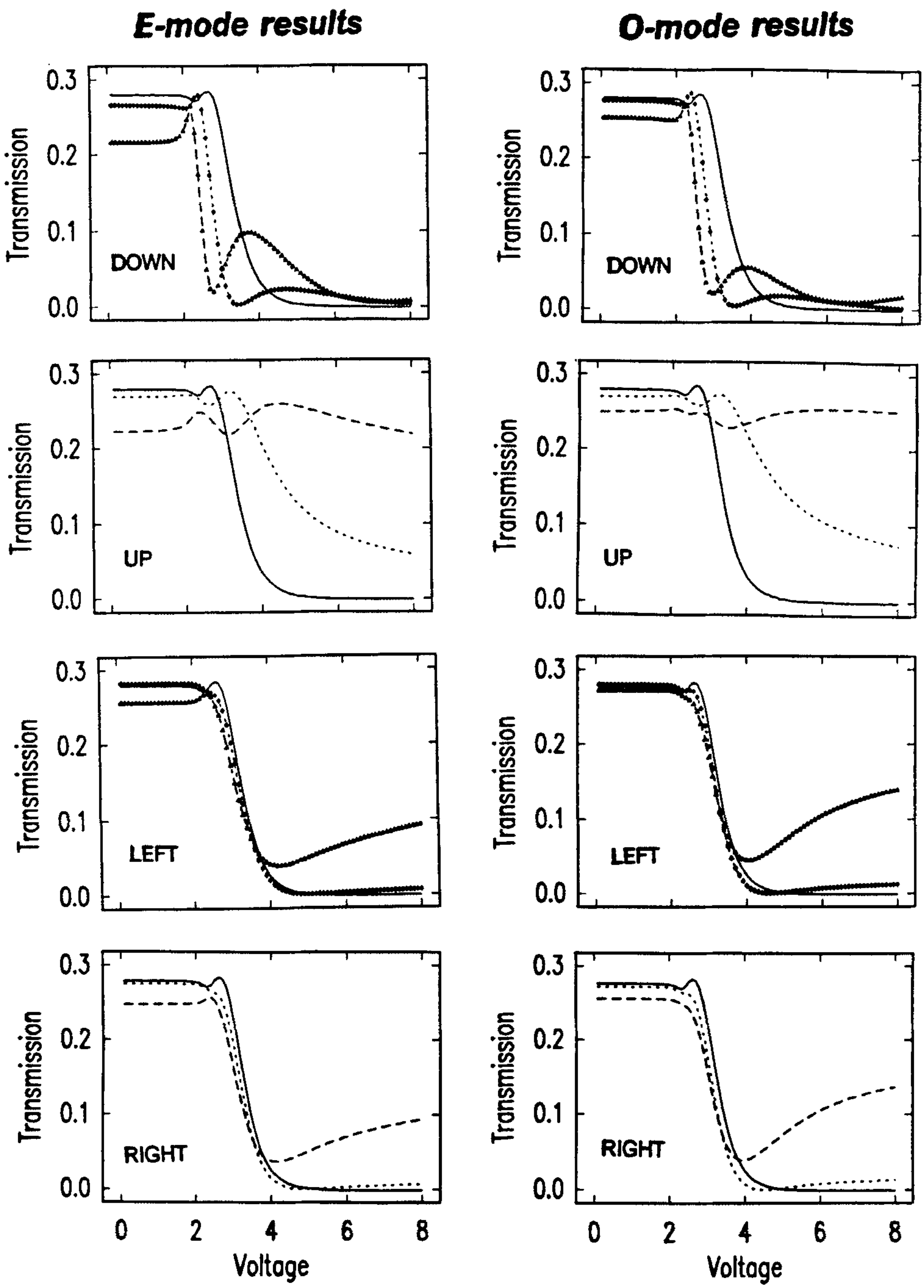

FIGURE 4 The experimental transmission versus applied voltage curves for four different viewing zones for a 90° TN cell filled with ZLI-3771 in the NW configuration. The left hand side is for the *e*-mode results, while the right hand side is for the *o*-mode results. Each sub-figure shows three viewing angles: 0° (solid line), 20° (dotted line with or without diamond symbols), and 40° (dashed line with or without triangle symbols) with respect to the substrate normal.

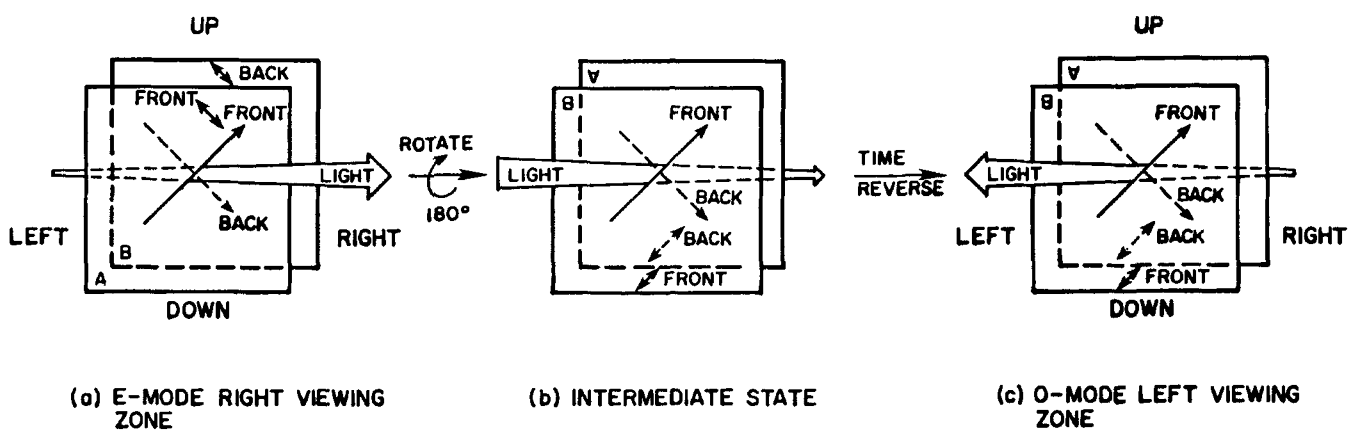

FIGURE 5 For the NB case, the *e*-mode right viewing zone is equivalent to the *o*-mode left viewing zone by rotation and time reversal transformations. The rubbing directions are shown with single head arrows, and the transmission axes of the polarizers are shown with double head arrows.

Figure 5(a), light is coming from the back on the left side to the front on the right side. Since the panel is viewed on the right side from the front, conventionally it is called the right viewing zone. The transmission axis of the entrance polarizer is parallel to the rubbing direction of the entrance surface, thus it is the e-mode configuration. Also, the transmission axes of two polarizers are parallel, it is a NB cell. Now, if we rotate the whole system, which includes the whole TN cell and the light source, 180° with respect to a horizontal axis as indicated, we obtain Figure 5(b). Notice that this rotation preserves the rubbing direction, and thus preserves the tilt direction of the LC director in the middle plane of the cell. In other words, the mid-plane LC directors in both Figure 5(a) and (b) are tilted toward the lower edge of the panel. Also, after rotation, the NB configuration stays the same as before. However, light now is going from the top on the left side into the back on the right side. We now reverse the propagation direction of light and obtain Figure 5(c). We now have the o-mode left viewing zone, since the transmission axis of the entrance polarizer is now perpendicular to the rubbing direction of the entrance surface, and we are viewing the panel on the left side from the front. Thus, we have proven that

$$\text{The } e\text{-mode right} \Leftrightarrow \text{The } o\text{-mode left.}$$

By the similar argument, we can prove that

$$\text{The } e\text{-mode left} \Leftrightarrow \text{The } o\text{-mode right.}$$

Using Figure 6, we can prove that

$$\text{The } e\text{-mode up} \Leftrightarrow \text{The } o\text{-mode up.}$$

By the similar argument, we can prove that

$$\text{The } e\text{-mode down} \Leftrightarrow \text{The } o\text{-mode down.}$$

For the NW case, using Figure 7 we can prove that

$$\text{The } e\text{-mode right} \Leftrightarrow \text{The } e\text{-mode left.}$$

By the similar argument, we can prove that

$$\text{The } o\text{-mode right} \Leftrightarrow \text{The } o\text{-mode left.}$$

So far, we have proven that Equations (1) and (2) hold for any 90° TN cell regardless of the cell gap thickness and the value of the pretilt angle.

From Figure 8, rotation and time reversal transformations give us that

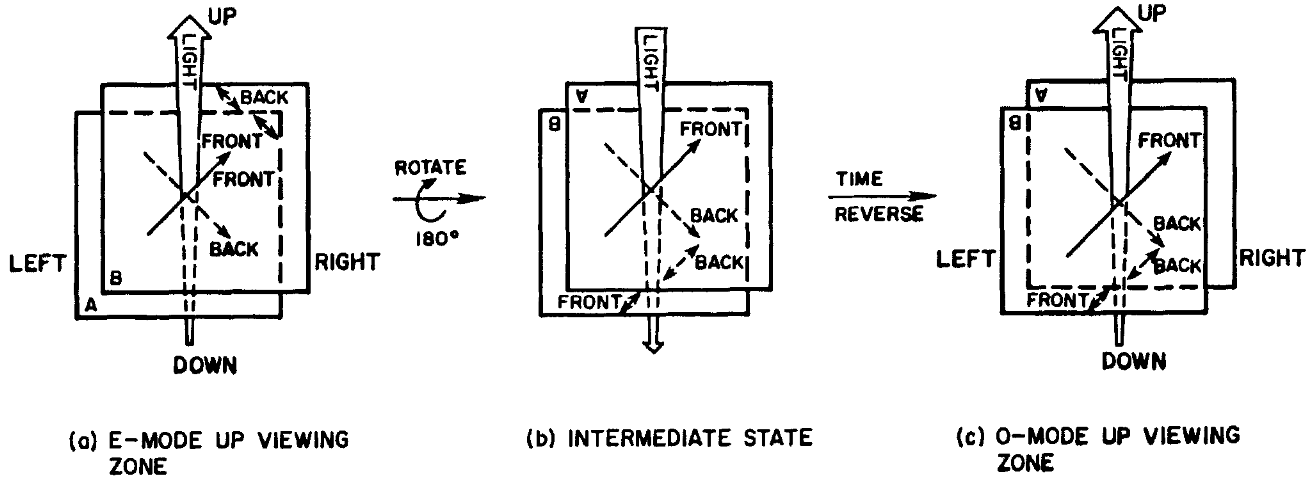

FIGURE 6 For the NB case, the *e*-mode up viewing zone is equivalent to the *o*-mode up viewing zone by rotation and time reversal transformations. The rubbing directions are shown with single head arrows, and the transmission axes of the polarizers are shown with double head arrows.

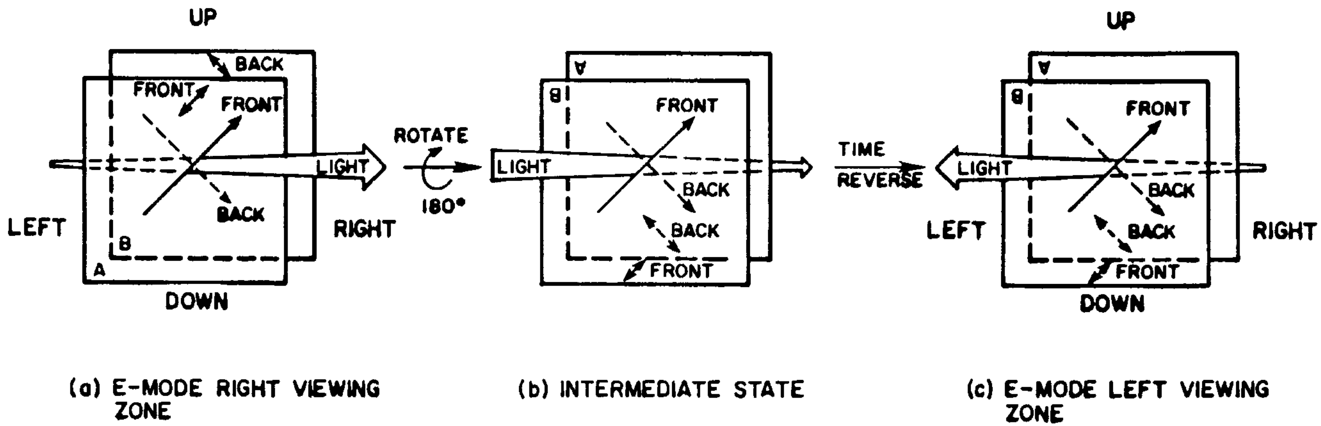

FIGURE 7 For the NW case, the *e*-mode right viewing zone is equivalent to the *e*-mode left viewing zone by rotation and time reversal transformations. The rubbing directions are shown with single head arrows, and the transmission axes of the polarizers are shown with double head arrows.

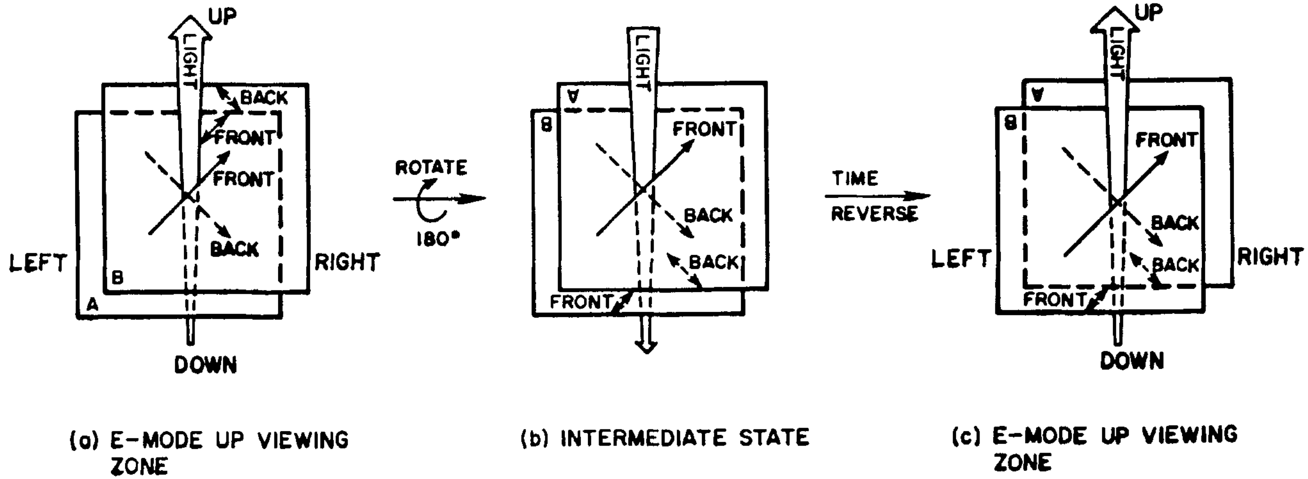

FIGURE 8 For the NW case, the *e*-mode up viewing zone is equivalent to the *e*-mode up viewing zone by rotation and time reversal transformations. The rubbing directions are shown with single head arrows, and the transmission axes of the polarizers are shown with double head arrows.

The e-mode up $\Leftrightarrow$ The e-mode up.

Similarly, we have that

The e-mode down $\Leftrightarrow$ The e-mode down,

The o-mode up $\Leftrightarrow$ The o-mode up,

The o-mode down $\Leftrightarrow$ The o-mode down.

These four transformations are all identity transformations. They imply that each figure in the up and down viewing zones for the NW case is totally independent. We cannot obtain any figure in those two viewing zones from any other figure by the above rotation and time reversal transformations.

V. CONCLUSION

In conclusion, we have discovered a set of symmetry properties of a 90° TN cell under rotation of polarizers both experimentally and theoretically. These symmetry properties can be explained by the argument based on rotation and time reversal transformations. By this argument, a viewing zone in the e-mode can be transformed into the corresponding viewing zone in the o-mode for the NB case. Taking all four viewing zones into account, the optical performance for the e-mode and o-mode are equivalent for the NB case. However, for the NW case, a viewing zone in the e-mode (or o-mode) is transformed into the corresponding viewing zone in the same mode. Thus, the e-mode and o-mode are not transformable and they are basically different, even for the normal incident case. These symmetry properties are very useful, since they provide us a quick test for any existing LCD computer simulation programs. If an LCD simulation program does not produce these symmetry results, it is certain that there is something wrong with the program, which must be corrected before it can be used. Furthermore, this rotation and time reversal transformations can be applied to the 0°, 180°, and 270° cells to obtained the corresponding symmetry properties for these cells.

Acknowledgment

The authors gratefully acknowledge Dr. W. E. Howard for several useful discussion and encouragements. We also benefited from discussions with Dr. K. H. Yang.

References

1. C. W. Oseen, *Trans. Faraday Soc.*, **29**, 883 (1933); F. C. Frank, Discuss. *Faraday Soc.*, **29**, 945 (1958); P. G. deGennes, "The Physics of Liquid Crystals," Oxford University Press, Oxford (1975).
2. D. W. Berreman, *Appl. Phys. Lett.*, **25**, 12 (1974) and erratum: *Appl. Phys. Lett.*, **25**, 321 (1974).
3. D. W. Berreman, *J. Opt. Soc. Am.*, **62**, 502 (1972); H. Wöhler, G. Haas, M. Fritsch and D. A. Mlynski, *J. Opt. Soc. Am. A.*, **5**, 1554 (1988).
4. G. Haas, H. Wöhler, M. Fritsch and D. A. Mlynski, *J. Opt. Soc. Am. A.*, **5**, 1571 (1988).